NASA TECHNICAL NOTE

NASA TN D-7942

FORMULATION OF THE INFORMATION CAPACITY OF THE OPTICAL-MECHANICAL LINE-SCAN IMAGING PROCESS

Friedrich O. Huck and Stephen K. Park

Langley Research Center
Hampton, Va. 23665

NATIONAL AERONAUTICS AND SPACE ADMINISTRATION • WASHINGTON, D. C. • AUGUST 1975

1. Report No.	2. Government Accession No.	3. Recipient's Catalog No.
NASA TN D-7942		

4. Title and Subtitle

FORMULATION OF THE INFORMATION CAPACITY OF THE OPTICAL-MECHANICAL LINE-SCAN IMAGING PROCESS

5. Report Date: August 1975

6. Performing Organization Code:

7. Author(s)

Friedrich O. Huck and Stephen K. Park

8. Performing Organization Report No.: L-10118

9. Performing Organization Name and Address

NASA Langley Research Center
Hampton, Va. 23665

10. Work Unit No.: 506-18-21-02

11. Contract or Grant No.:

12. Sponsoring Agency Name and Address

National Aeronautics and Space Administration
Washington, D.C. 20546

13. Type of Report and Period Covered: Technical Note

14. Sponsoring Agency Code:

15. Supplementary Notes

16. Abstract

An expression for the information capacity of the optical-mechanical line-scan imaging process is derived which includes the effects of blurring of spatial detail, photosensor noise, aliasing, and quantization. Both the information capacity for a fixed data density and the information efficiency (i.e., the ratio of information capacity to data density) exhibit a distinct single maximum when displayed as a function of sampling rate, and the location of this maximum is determined by the system frequency-response shape, signal-to-noise ratio, and quantization interval.

17. Key Words (Suggested by Author(s))

Information capacity and efficiency
Optical-mechanical line-scan imaging process
Facsimile camera
Aliasing

18. Distribution Statement

Unclassified – Unlimited

New Subject Category 35

19. Security Classif. (of this report)	20. Security Classif. (of this page)	21. No. of Pages	22. Price*
Unclassified	Unclassified	35	$3.75

*For sale by the National Technical Information Service, Springfield, Virginia 22161

FORMULATION OF THE INFORMATION CAPACITY OF THE OPTICAL-MECHANICAL LINE-SCAN IMAGING PROCESS

Friedrich O. Huck and Stephen K. Park
Langley Research Center

SUMMARY

The information capacity of the optical-mechanical line-scan imaging process is formulated by generally following the classical work of Fellgett and Linfoot who applied Shannon's theory of information to the assessment of film-camera images. Although images obtained with film cameras and optical-mechanical line-scan devices are both degraded by blurring of spatial detail and by noise, the latter images are also degraded by aliasing that results when spatial scene radiance variations are undersampled, and by quantization that results when the photosensor analog signal is converted to a digital signal for transmission.

Numerical evaluations of the derived expression reveal that both the information capacity for a fixed data density and the information efficiency (i.e., the ratio of information capacity to data density) exhibit a distinct single maximum when displayed as a function of sampling rate, and that the location of this maximum is determined by the system frequency-response shape, signal-to-noise ratio, and quantization interval. These results suggest a general design criteria for optical-mechanical line-scan devices: namely, the optimization of either their information capacity for a fixed data density or their information efficiency, especially if large quantities of data are involved or the data must be transmitted over long distances.

INTRODUCTION

Film and television cameras have generally been employed in the past to characterize spatial variations of scene brightness, whereas optical-mechanical line-scan devices have been employed to characterize spectral and radiometric variations. Little attention has, therefore, been paid to the image quality of spatial detail obtained with the latter devices. However, the spatial characterization of scenes has become in recent years an important objective in several applications of the optical-mechanical line-scan technique to multispectral imaging systems for Earth-orbiting spacecraft; and it is the most important objective in applications to the so-called facsimile cameras of the U.S.S.R. spacecraft Luna (ref. 1) and Lunakhod (ref. 2) and the U.S. spacecraft Viking Lander (ref. 3).

Data returned from Earth-orbiting spacecraft are constantly increasing, and data returned from planetary spacecraft will remain very expensive. In both cases, the quality of the data is most generally assessed by its information content, and the capability of the imaging system by its information capacity. The application of information theory to the assessment of optical-mechanical line-scan devices is particularly interesting because the quantity of data that is transmitted and the quantity of information that these data can contain are interrelated by two factors: the inevitable line-scan sampling process associated with this device, and the electronic sampling and quantization process required for digital data transmission.

The approach that is pursued here to formulate the information capacity of the optical-mechanical line-scan imaging process generally follows the classical work of Fellgett and Linfoot (ref. 4) who applied Shannon's theory of information (ref. 5) to the assessment of the image quality obtained with film cameras. Images obtained with film cameras and optical-mechanical line-scan devices are both degraded by blurring of small detail and by random noise. However, the latter images are also degraded by the aliasing that results when spatial scene radiance variations are undersampled and by the quantization that results when the photosensor analog signal is converted to a digital signal for transmission.

SYMBOLS

A	isoplanatism patch of camera field of view
$\|A\|$	solid angle of isoplanatism patch, sr
$\hat{B}$	sampling frequency passband
$\hat{F}$	camera frequency passband
$g(\chi,\psi)$	spatial function confined to A
$\hat{g}(\upsilon,\omega)$	frequency spectrum of $g(\chi,\psi)$ confined to $\hat{F}$
h_d	data density, bits/sr
h_i	information density or capacity, binits/sr
H_d	quantity of data in A, bits

H_g	entropy of $g(\chi,\psi)$, binits
H_i	quantity of information in A, binits
$I(\chi,\psi)$	random variable, minus its average value, of all signal and noise components in A
k	filter-shape parameter (see fig. 3)
K	average signal, A
m,n	elevation and azimuth sampling counts, respectively
M,N	number of elevation and azimuth samples, respectively
n_e	magnitude of white Gaussian noise spectrum, A
$N(\chi,\psi)$	random variable, minus its average value, of all noise components in A
$\bar{N}(\lambda)$	average spectral radiance of object, W/m^2-sr-μm
$o(\chi,\psi)$	normalized spatial distribution of object radiance
p,q	elevation and azimuth integers of mathematical sampling points in $\hat{F}$, respectively
$P(\chi,\psi)$	random variable, minus its average value, of all signal components in A
$S(\chi,\psi)$	spatial distribution of camera signal, A
$\hat{S}(\upsilon,\omega)$	frequency spectrum of camera signal, A
X,Y	elevation and azimuth sampling intervals, respectively, rad
δ	delta or unit impulse function
η	number of binary encoding levels, bits
κ	number of quantization levels

λ	wavelength, μm
σ	standard deviation
$\tau(\chi,\psi)$	point-spread function
$\hat{\tau}(\upsilon,\omega)$	spatial frequency response
υ,ω	elevation and azimuth spatial frequencies, respectively, rad^{-1}
υ_e	cutoff frequency of electronic filter, rad^{-1}
$\hat{\Upsilon}(\upsilon,\omega)$	square root of $\hat{\tau}(\upsilon,\omega)$
$\hat{\phi}(\upsilon,\omega)$	Wiener spectrum, or power spectral density
χ,ψ	elevation and azimuth angles of camera scanning coordinates, respectively, rad
$\amalg(\chi,\psi)$	sampling or comb function
$(\bar{\ })$	average value or ensemble average
$(\hat{\ })$	spatial frequency domain
$(\ )*(\ )$	convolution

Subscripts:

an	aliasing noise
c	camera
e	electronics
en	electronic noise
g	spatial function $g(\chi,\psi)$
l	lens

o optics

ps proper signal

FORMULATION

The Optical-Mechanical Line-Scan Imaging Process

Consider an optical-mechanical line-scan imaging device such as the facsimile camera shown in figure 1. Radiation from the object field is reflected by the scanning mirror, captured by the objective lens, and projected onto a plane which contains a photosensor covered by a small aperture. The photosensor converts the radiation falling on the aperture into an electrical signal which is then amplified, sampled, and quantized for digital transmission. As the mirror rotates, the imaged object field moves past the aperture and thus permits the aperture to scan vertical strips. The camera rotates in small steps between each vertical line scan until the entire object field of interest is scanned. The distance between object and camera is assumed to be large compared with the distance between camera mirror and lens; thus, spherical coordinates with an origin at the center of the objective lens can be used as reference for the elevation and azimuth imaging coordinates, labeled "χ" and "ψ," respectively.

The process by which this device transfers the (continuous) object radiance distribution $o(\chi,\psi)$ into a (discrete) electrical signal $S(\chi,\psi)$ can be approximately formulated by the equation (ref. 6)

$$S(\chi,\psi) = K\left[o(\chi,\psi) * \tau_c(\chi,\psi)\right] \text{Ш}\left(\frac{\chi}{X},\frac{\psi}{Y}\right) \tag{1}$$

The symbol $*$ denotes convolution, K is the camera response to uniform radiance, and $\tau_c(\chi,\psi)$ is the camera point-spread function which, in turn, is given by

$$\tau_c(\chi,\psi) = \tau_l(\chi,\psi) * \tau_p(\chi,\psi) * \left[\tau_e(\chi)\ \delta(\psi)\right]$$

where $\tau_l(\chi,\psi)$, $\tau_p(\chi,\psi)$, and $\tau_e(\chi)\ \delta(\psi)$ are the point-spread functions of the lens, photosensor aperture, and signal electronics, respectively. The symbol $\text{Ш}\left(\frac{\chi}{X},\frac{\psi}{Y}\right)$ is the sampling (ref. 7) or comb (ref. 8) function. This function is an infinite sum of delta functions with spacings X and Y radians, which in this case correspond to the effective camera elevation and azimuth sampling intervals, respectively:

$$\text{Ш}\left(\frac{\chi}{X},\frac{\psi}{Y}\right) = \sum_{m=-\infty}^{\infty}\sum_{n=-\infty}^{\infty} \delta\left(\frac{\chi}{X}-m,\frac{\psi}{Y}-n\right) = XY \sum_{m=-\infty}^{\infty}\sum_{n=-\infty}^{\infty} \delta(\chi-Xm,\psi-Yn)$$

For facsimile cameras used on planetary landers, the spacing Y is equal to the azimuth stepping interval times the cosine of χ where χ is measured from a plane normal to the optical axis of the objective lens.

An approximation is introduced into the formulation of equation (1) by the separation of spectral and spatial object and camera characteristics, with the average signal K accounting for the spectral characteristics. Actually, $o(\chi,\psi)$ and $\tau_c(\chi,\psi)$ are functions of wavelength, and the spatial convolution should, therefore, be integrated over wavelength. However, it is convenient here to let (ref. 9)

$$K = A_c B_c \int_0^\infty \bar{N}(\lambda)\, \tau_c(\lambda)\, R(\lambda)\, d\lambda \tag{2}$$

where A_c is the area of the lens aperture, B_c is the solid angle of the field of view formed by the photosensor aperture (i.e., the solid angle that defines a picture element), $\bar{N}(\lambda)$ is the average spectral radiance of the object, $\tau_c(\lambda)$ is the transmittance of the camera optics, and $R(\lambda)$ is the responsivity of the photosensor. The use of K in equation (1) permits $o(\chi,\psi)$ and $\tau_c(\chi,\psi)$ to be expressed as normalized functions while $S(\chi,\psi)$ takes on the unit of K, which is amperes.

The optical-mechanical line-scan imaging process is implicitly a function of time. The formulation of equation (1) implies, therefore, that the convolution of the object radiance distribution with the camera point-spread function be performed for each picture element (pixel) in a picture to allow for changes of $o(\chi,\psi)$ or $\tau_c(\chi,\psi)$ with time. If neither object radiance distribution nor camera response varies with time (as is assumed here), then it is immaterial whether the pixels in a picture are formed simultaneously or in sequence, and the convolution needs to be performed only once for each picture.

Significant variations in defocus blur and in azimuth sampling intervals, however, may occur as a function of the elevation scanning angle. If such variations occur, it is necessary for the purpose of analysis to divide the camera field of view into isoplanatism patches (i.e., areas within which these variations become negligibly small) and restrict all formulations to such a patch. The total information contained in an image is the sum of the information contained in all the patches that make up the image.

An isoplanatism patch is denoted here by A and assumed to be rectangular and centered at $\chi = \psi = 0$. For M samples per line scan and N line scans in A, χ, and ψ are limited to

$$-XM/2 \leqq \chi \leqq XM/2$$

$$-YN/2 \leqq \psi \leqq YN/2$$

and the solid angle subtended by A is $|A| = XYMN$ steradians. Any spatial function $g(\chi,\psi)$ is then said to be confined to A if $g(\chi,\psi) = 0$ for all points outside A. The error that is introduced by confining the radiance distribution $o(\chi,\psi)$ to A is negligibly small everywhere in A except at a very narrow strip along the boundary of A. (See, for example, refs. 10 and 11.)

The imaging process formulated by equation (1) is generally more convenient to evaluate for the isoplanatism patch A in the frequency rather than spatial domain. Any spatial function $g(\chi,\psi)$ which is confined to A and its corresponding frequency function $\hat{g}(\upsilon,\omega)$ are related by the Fourier transform pair

$$\hat{g}(\upsilon,\omega) = \iint_A g(\chi,\psi) e^{-i2\pi(\upsilon\chi+\omega\psi)} d\chi\, d\psi$$

$$g(\chi,\psi) = \int_{-\infty}^{\infty}\int \hat{g}(\upsilon,\omega) e^{i2\pi(\upsilon\chi+\omega\psi)} d\upsilon\, d\omega$$

By using this transformation, equation (1) becomes

$$\hat{S}(\upsilon,\omega) = K\left[\hat{o}(\upsilon,\omega)\,\hat{\tau}_c(\upsilon,\omega)\right] * XY\,\text{⫼}(X\upsilon,Y\omega) \tag{3a}$$

where

$$\hat{\tau}_c(\upsilon,\omega) = \hat{\tau}_l(\upsilon,\omega)\,\hat{\tau}_p(\upsilon,\omega)\,\hat{\tau}_e(\upsilon)$$

and

$$XY\,\text{⫼}(X\upsilon,Y\omega) = \sum_{m=-\infty}^{\infty}\sum_{n=-\infty}^{\infty} \delta\left(\upsilon - \frac{m}{X}, \omega - \frac{n}{Y}\right)$$

Equation (3a) can be written more conveniently as

$$\hat{S}(\upsilon,\omega) = K \sum_{m=-\infty}^{\infty}\sum_{n=-\infty}^{\infty} \hat{o}\left(\upsilon - \frac{m}{X}, \omega - \frac{n}{Y}\right)\hat{\tau}_c\left(\upsilon - \frac{m}{X}, \omega - \frac{n}{Y}\right) \tag{3b}$$

or

$$\hat{S}(\upsilon,\omega) = K\,\hat{o}(\upsilon,\omega)\,\hat{\tau}_c(\upsilon,\omega) + K \sum_{\substack{m=-\infty \\ (m,n)\neq(0,0)}}^{\infty}\sum_{n=-\infty}^{\infty} \hat{o}\left(\upsilon - \frac{m}{X}, \omega - \frac{n}{Y}\right)\hat{\tau}_c\left(\upsilon - \frac{m}{X}, \omega - \frac{n}{Y}\right) \tag{3c}$$

The first term of the equation for $\hat{S}(\upsilon,\omega)$ given by equation (3c), $K\,\hat{o}(\upsilon,\omega)\,\hat{\tau}_c(\upsilon,\omega)$, is equal to the image frequency spectrum obtained with film cameras if $\hat{\tau}_c(\upsilon,\omega)$ is interpreted as the combined camera lens and film spatial frequency response and K as a (linear) film exposure-to-density transfer function. It is the existence of the sidebands given by the second term in equation (3c) that distinguishes the signal frequency spectrum generated by the optical-mechanical line-scan imaging process from the image frequency spectrum of the film camera.

In order to characterize the signal frequency spectrum $\hat{S}(\upsilon,\omega)$, it is convenient to make the following two definitions: First, let $\hat{F}$ be the camera passband; ultimately, this passband is limited by the diffraction limit of the camera objective lens $\left(\text{i.e., } \upsilon^2 + \omega^2 < \left(\frac{2 \sin \alpha}{\lambda}\right)^2, \text{ where } \sin \alpha \text{ is the lens numerical aperture}\right)$. Second, let $\hat{B}$ be the sampling passband with corner points $\upsilon = \pm\frac{1}{2X}$ and $\omega = \pm\frac{1}{2Y}$ and sides parallel to the frequency coordinates (υ,ω). Two cases must be recognized as illustrated in figure 2: (a) sufficient sampling when $\hat{F} \subset \hat{B}$; and (b) insufficient sampling, or undersampling, when $F \not\subset B$.

If sufficient sampling occurs (fig. 2(a)), then the "proper signal" term $K\,\hat{o}(\upsilon,\omega)\,\hat{\tau}_c(\upsilon,\omega)$ can, in the absence of noise, be completely recovered by passing the signal frequency spectrum through an ideal low-pass filter whose passband agrees with the camera passband $\hat{F}$ or sampling passband $\hat{B}$. However, if insufficient sampling occurs (fig. 2(b)), then the "proper signal" components cannot be completely recovered, because displaced, false-frequency components, called aliased signals, fall into the passband $\hat{F}$. These aliased signal components cannot be distinguished in practice from the proper-signal components but tend to mask spatial detail in the image just like noise. The aliased signal is consequently treated as noise whose power is additive.

Data Density

Recall that M is the number of samples per line scan and N is the number of line scans in the isoplanatism patch A, and let κ be the number of quantization levels of each sample. Then, the number of distinguishable states in A is κ^{MN}, and the amount of data in A is given by

$$H_d = MN \log_2 \kappa = \frac{|A|}{XY} \log_2 \kappa$$

The units of H_d are binary digits. It follows that the data density in A $\left(\text{i.e., the channel capacity of the optical-mechanical line-scan device for the field of view } |A|\right)$ is given by

$$h_d = \frac{H_d}{|A|} = \frac{1}{XY} \log_2 \kappa \tag{4a}$$

The units of h_d are binary digits per steradian. For η-bit encoding, $\kappa = 2^\eta$ and

$$h_d = \frac{\eta}{XY} \tag{4b}$$

If all the image states κ^{MN} are independent and equally probable, then H_d is the amount of information contained in A and h_d is the information density. However, all image states are generally neither independent nor equally probable in practice. To distinguish between units of data and information, the unit "binary digits" will be abbreviated to "bits" for data and to "binits" for information.

Information Density

The spatial radiance distribution of natural scenes is generally not completely predictable and must be treated as a random phenomenon. Otherwise, of course, the image data of such a scene could not be considered to carry any information. Image data of a reference test chart, for example, are not intended to provide information about the chart but about the camera performance. Consequently, an imaging system (just like a communication or control system) must be designed for an ensemble of scene radiances (or messages) and an ensemble of noise, not a particular scene radiance (or message) and a particular realization of noise. Wiener has shown that power spectral density is a meaningful and useful statistical description of random phenomena (ref. 12). For optical systems, the power spectral density is often referred to as the Wiener spectrum to free the mathematical concept of a power spectral density from its physical implications in electrical engineering (ref. 13).

Before formulating these statistics for the optical-mechanical line-scan imaging process, it is convenient to review a general analytical representation of random phenomena as presented by Fellgett and Linfoot (ref. 4) and by Linfoot (ref. 10) for optical images. Pertinent scene and camera characteristics are then molded into this analytical presentation, leading directly to the desired formulation of the information density generated by the optical-mechanical line-scan imaging process.

Analytical representation.- Let the spatial function $g(\chi,\psi)$ be a random process that represents any signal or noise component confined to the isoplanatism patch A of the reconstructed line-scan image; let the Fourier transform of this function $\hat{g}(\upsilon,\omega)$ be the corresponding frequency spectrum confined to the camera passband $\hat{F}$; and let

$$\hat{\phi}_g(\upsilon,\omega) = \frac{1}{|A|} \overline{|\hat{g}(\upsilon,\omega)|^2} \tag{5}$$

be the corresponding Wiener spectrum. In other words, the Wiener spectrum can be calculated by averaging the modulus squared of the Fourier transform of $g(\chi,\psi)$, that is, $|\hat{g}(\upsilon,\omega)|^2$, over the ensemble to which $g(\chi,\psi)$ belongs and by dividing the result by the area $|A|$.

The function $g(\chi,\psi)$ is real for the case of incoherent radiation treated here, so that the complex conjugate of $\hat{g}(\upsilon,\omega)$ is equal to $\hat{g}(-\upsilon,-\omega)$. The Wiener spectrum is always real, nonnegative, and symmetric about the origin $\left(\text{i.e., } \hat{\phi}_g(\upsilon,\omega) = \hat{\phi}_g(-\upsilon,-\omega)\right)$.

Furthermore, let $\hat{g}_{pq} = \hat{g}\left(\upsilon_p,\omega_q\right)$ be the value of $\hat{g}(\upsilon,\omega)$ at the sampling points $\left(\upsilon_p,\omega_q\right) = (p/XM,q/YN)$, where p and q are integers. The sampling intervals $(1/XM,1/YN)$ assure sufficient (mathematical) sampling since $g(\chi,\psi)$ is confined to A (i.e., $|\chi| \leq XM/2, |\chi| \leq YN/2$). The frequency function $\hat{g}(\upsilon,\omega)$ can then be reconstructed from the sampled values according to Shannon's sampling theorem (ref. 5)

$$\hat{g}(\upsilon,\omega) \approx \sum_{pq \in \hat{F}} \sum \hat{g}_{pq} \operatorname{sinc}(XM\upsilon - p) \operatorname{sinc}(YN\omega - q)$$

where

$$\operatorname{sinc} \upsilon = \frac{\sin \pi\upsilon}{\pi\upsilon}$$

and the notation $pq \in \hat{F}$ indicates that the summation is performed over all sampling points in $\hat{F}$. The spatial function $g(\chi,\psi)$ can be reconstructed by the Fourier series expansion

$$g(\chi,\psi) = \begin{cases} \dfrac{1}{|A|} \displaystyle\sum_{pq \in F} \sum \hat{g}_{pq}\, e^{2\pi i\left(\frac{p\chi}{XM} + \frac{q\psi}{YN}\right)} & ((\chi,\psi) \in A) \\ 0 & ((\chi,\psi) \notin A) \end{cases}$$

To avoid possible confusion it should be pointed out that the sampling intervals $(1/XM,1/YN)$ in the frequency domain are not directly related to the camera sampling intervals (X,Y) in the spatial domain except through the somewhat arbitrarily defined solid angle $|A|$ of the isoplanatism patch A. The former sampling intervals are introduced to provide a convenient analytical representation of scene and camera characteristics as a summation of discrete sampling values. The latter sampling intervals are an inherent aspect of the optical-mechanical line-scan imaging process.

The statistical properties of any signal or noise component $g(\chi,\psi)$ confined to A can be characterized by the statistical properties of the finite collection of complex random

variables $\hat{g}_{pq}$ for which $(\upsilon_p,\omega_q) \in \hat{F}$. If $\hat{g}_{pq}$ has a probability distribution $p_{pq}(\hat{g})$, the entropy of $\hat{g}_{pq}$ is defined as

$$H_{\hat{g}_{pq}} = -\iint p_{pq}(\hat{g}) \log_2 p_{pq}(\hat{g})\, d\zeta\, d\xi \tag{6}$$

where ζ and ξ are the real and imaginary components of $\hat{g}_{pq}$, respectively. Due to the conjugate symmetry of the collection of $\hat{g}_{pq}$, only one-half of them can be assumed to be independent. With this understanding, the joint entropy of the collection of $\hat{g}_{pq}$ (i.e., of $\hat{g}(\upsilon,\omega)$) is given by

$$H_g = \frac{1}{2} \sum\sum_{pq \in \hat{F}} H_{\hat{g}_{pq}} \tag{7}$$

Each sample value of $\hat{g}_{pq}$ is assumed to have a Gaussian (i.e., normal) probability density function with mean zero and variance $\sigma^2_{g,pq}$ equal to the average power of $\hat{g}_{pq}$; that is,

$$p_{pq}(\hat{g}) = \frac{1}{2\pi\sigma^2_{g,pq}} e^{-|\hat{g}|^2 / 2\sigma^2_{g,pq}} \tag{8}$$

where

$$\sigma^2_{g,pq} = \frac{1}{A} \hat{\phi}_g(\upsilon_p,\omega_q)$$

For a random variable with a specified variance, the Gaussian probability density function represents the maximum statistical uncertainty, or entropy, of the random variable. Substituting this function into equations (6) and (7) yields the following familiar results (ref. 5):

$$H_{\hat{g}_{pq}} = \log_2 4\pi\sigma^2_{g,pq} \tag{9}$$

$$H_g = \frac{1}{2} \sum\sum_{pq \in \hat{F}} \log_2 4\pi\sigma^2_{g,pq} \tag{10}$$

Now, let the spatial function $I(\chi,\psi)$ be the random variable, minus its average value, that represents all the signal and noise components that have been constructed (without loss of information) in the isoplanatism patch A of the image; let the Fourier

transform of this function $\hat{I}(\upsilon,\omega)$ be the corresponding frequency spectrum confined to the camera passband $\hat{F}$; and let $\hat{\phi}_I(\upsilon,\omega)$ be the corresponding Wiener spectrum. Similarly, let $P(\chi,\psi)$ be the signal components of $I(\chi,\psi)$, minus its average value, with $\hat{P}(\upsilon,\omega)$ and $\hat{\phi}_P(\upsilon,\omega)$ the corresponding frequency and Wiener spectrum, respectively; and let $N(\chi,\psi)$ be the noise components of $I(\chi,\psi)$, with $\hat{N}(\upsilon,\omega)$ and $\hat{\phi}_N(\upsilon,\omega)$ the corresponding frequency and Wiener spectrum, respectively. It is assumed that the signal and noise components are additive and statistically independent, so that

$$\sigma^2_{I,pq} = \sigma^2_{P,pq} + \sigma^2_{N,pq}$$

In the sense that the information gained about a scene can be regarded as a reduction in the statistical uncertainty, or entropy, about the probable state of the scene, the quantity of information H_i contained in $I(\chi,\psi)$ is defined within the foregoing constraints as

$$H_i = H_I - H_N = \frac{1}{2}\sum\sum_{pq\in\hat{F}} \log_2 4\pi\sigma^2_{I,pq} - \frac{1}{2}\sum\sum_{pq\in\hat{F}} \log_2 4\pi\sigma^2_{N,pq}$$

$$H_i = \frac{1}{2}\sum\sum_{pq\in\hat{F}} \log_2 \frac{\sigma^2_{I,pq}}{\sigma^2_{N,pq}} = \frac{1}{2}\sum\sum_{pq\in\hat{F}} \log_2 \left(1 + \frac{\sigma^2_{P,pq}}{\sigma^2_{N,pq}}\right) \tag{11}$$

This summation can be approximated by an integration of a continuous function over $\hat{F}$ as

$$H_i = \frac{1}{2}|A| \iint_{\hat{F}} \log_2 \left[1 + \frac{\hat{\phi}_P(\upsilon,\omega)}{\hat{\phi}_N(\upsilon,\omega)}\right] d\upsilon\, d\omega$$

The information density in the isoplanatism patch A is then given by

$$h_i = \frac{H_i}{|A|} = \frac{1}{2}\iint_{\hat{F}} \log_2 \left[1 + \frac{\hat{\phi}_P(\upsilon,\omega)}{\hat{\phi}_N(\upsilon,\omega)}\right] d\upsilon\, d\omega \tag{12}$$

The units of h_i are binits per steradians.

Object radiance.- The radiance distribution of a natural scene is taken to be $\bar{N}(\lambda)\, o(\chi,\psi)$ with the spectral and spatial characteristics separated for convenience. The spatial characteristics are given by the random variable $o(\chi,\psi)$ which has the following

two constraints: (1) The variations of $o(\chi,\psi)$ are effectively confined to the range

$$\left.\begin{aligned} 0 \leqq o(\chi,\psi) \leqq 2 \qquad & ((\chi,\psi) \in A) \\ o(\chi,\psi) = 0 \qquad & ((\chi,\psi) \notin A) \end{aligned}\right\} \tag{13}$$

(2) The average value of $o(\chi,\psi)$ is unity; that is,

$$\frac{1}{|A|}\iint_A o(\chi,\psi)\,d\chi\,d\psi = 1 \tag{14}$$

An ensemble of scenes may be regarded to contain all scenes that consist of the same composition and have undergone the same morphological processes. The information content of the scene is contained in the spatial distribution $o(\chi,\psi)$ of the radiance. However, it should be recognized that the average photosensor signal K is proportional to the spatial average value of the scene radiance $\overline{N}(\lambda)$ (see eq. (2)) and that $\overline{N}(\lambda)$ contributes, therefore, to the amount of information about the scene that can ultimately be recovered from the camera signal. With this understanding, the Wiener spectrum of the scene is defined as

$$\hat{\phi}_o(\upsilon,\omega) = \frac{1}{|A|}\overline{|\hat{o}(\upsilon,\omega)|^2} \tag{15}$$

where again $\overline{|\hat{o}(\upsilon,\omega)|^2}$ indicates that $|\hat{o}(\upsilon,\omega)|^2$ has been averaged over the ensemble to which $\hat{\phi}(\upsilon,\omega)$ belongs.

Camera signal.- The Wiener spectrum of the camera signal is defined as

$$\hat{\phi}_s(\upsilon,\omega) = \frac{1}{|A|}\overline{|\hat{S}(\upsilon,\omega)|^2}$$

where $\hat{S}(\upsilon,\omega)$ is given by equations (3). It is assumed on practical grounds that the aliased signals are to be treated as noise – similar, for example, to the noise generated by the photosensor. It may be pointed out to emphasize this analogy that the Wiener spectrum of the aliased signal, like that of the photosensor noise, may be assumed known; but a particular realization of either aliased signal or photosensor noise cannot be assumed known for any random process. The Wiener spectrum of the "proper signal" $\hat{\phi}_{ps}(\upsilon,\omega)$ (i.e., of that component which is contained in the camera passband $\hat{F}$ when sufficient sampling occurs) is defined as

$$\hat{\phi}_{ps}(\upsilon,\omega) = K^2\,\hat{\phi}_o(\upsilon,\omega)\left|\hat{\tau}_c(\upsilon,\omega)\right|^2 \tag{16}$$

Following Blackman and Tukey (ref. 14), the Wiener spectrum of the "aliased noise" $\hat{\phi}_{an}(\upsilon,\omega)$ (i.e., of those components that are contained in $\hat{F}$ only when insufficient sampling occurs) is defined as

$$\hat{\phi}_{an}(\upsilon,\omega) = K^2 \sum_{\substack{m=-\infty \\ (m,n)\neq(0,0)}}^{\infty} \sum_{n=-\infty}^{\infty} \hat{\phi}_o\left(\upsilon - \frac{m}{X}, \omega - \frac{n}{Y}\right) \left|\hat{\tau}_c\left(\upsilon - \frac{m}{X}, \omega - \frac{n}{Y}\right)\right|^2 \tag{17}$$

Electronic noise.- Noise is present in the object radiation itself, in the photosensor which transduces this radiation into an electrical signal, and in the electronic circuit which amplifies the small photosensor current into a signal large enough to be processed for transmission. Noise in the object radiation, referred to as photon noise, results from the random arrival of photons at the photosensor. However, the magnitude of this noise is significantly smaller than the noise generated in the solid-state photosensors and associated electronics that would generally be used with optical-mechanical line-scan devices. The noise generated in photosensors can be divided into noise affected in magnitude by the presence of the arriving radiation, referred to as shot noise, and noise not so affected, referred to as dark current. The noise generated by the electronics is independent of the magnitude of the arriving radiation. It is generally too complicated to account rigorously for variations in shot noise as a function of variations in signal level; instead, an average value for the shot noise based on an average signal current K can readily be accounted for. This approximation applies in particular to low-contrast scenes.

The electronic noise is amplified and sampled together with the signal for digital transmission. Just as undersampling of the signal frequency spectrum generates aliasing, so does undersampling of the noise frequency spectrum generate additional noise. However, severe undersampling of the electronic-noise frequency spectrum that would generate a significant increase in the magnitude of the noise samples should generally be avoidable by proper shaping of the electronic frequency response $\hat{\tau}_e(\upsilon)$. The Wiener spectrum of the sampled noise at the output of the electronics becomes then

$$\hat{\phi}'_{en}(\upsilon) = \hat{\phi}_{en}(\upsilon)\left|\hat{\tau}_e(\upsilon)\right|^2 \tag{18}$$

where $\hat{\phi}_{en}(\upsilon)$ is the Wiener spectrum of the unfiltered electronic noise.

Quantization noise.- After the electrical signal (and noise) that has been generated along the line-scan direction is sampled, each one of the samples is also quantized for digital transmission. The quantization effect is a basic limitation of digital systems in determining the true value of a signal, just as random noise is a limitation of analog systems.

In order to determine the loss of information that results from quantization, it is necessary to account for some of the assumptions that have already been made about the signal and noise. Pertinent assumptions are: The average value of the signal is K and of the noise is zero; the probability density functions of signal and noise are Gaussian; and the effective range of signal variations is $2K$. To form a valid model of the quantization process with these assumptions, it is necessary to assume also that the average-signal-to-rms-noise ratio is large – say, 10 or more. (This constraint is not serious in practice since only extremely poor images are reproduced from signals for which the signal-to-noise ratio is less than 10.)

Additional assumptions are as follows: The signal is linearly quantized over its effective range $2K$, so that the quantum levels have a uniform spacing of $2K/\kappa$ where κ is the number of quantization levels; the quantization error of any one sample is uncorrelated with that of any other sample; and the signal occurs equally likely anywhere in the quantization interval $-K/\kappa$ to K/κ. The last assumption is valid only if the number of quantization intervals is large – say, $\kappa \geqq 16$ (i.e., 4-bit encoding or more).

These assumptions imply that the quantization error n_κ has the uniform probability density function (ref. 15)

$$p\left(n_\kappa\right) = \frac{\kappa}{2K} \qquad \left(-K/\kappa \leqq n_\kappa \leqq K/\kappa\right)$$

$$= 0 \qquad \text{(Elsewhere)}$$

In fact, a random variable which is constrained to a finite interval has maximum entropy when its probability density function is uniform.

A signal that is uniformly distributed between $-K/\kappa$ and K/κ has a mean equal to zero and a variance given by

$$\sigma^2_{\kappa n} = \int_{-K/\kappa}^{K/\kappa} n_\kappa^2 \, p\left(n_\kappa\right) \, dn_\kappa = \frac{K^2}{3\kappa^2}$$

Since quantization noise is uncorrelated (in the spatial domain), it has a Wiener spectrum equal to its variance; that is,

$$\hat{\phi}_{\kappa n}(\upsilon,\omega) = \frac{K^2}{3\kappa^2} \tag{19}$$

Quantization noise will be treated as additive white Gaussian noise with the Wiener spectrum given by equation (19). The fact that this treatment of quantization leads to reasonable results is demonstrated in the next section.

Formulation of information density.- It remains now only to recognize that $\hat{\phi}_P(\upsilon,\omega)$ in equation (12) is equal to the Wiener spectrum of the proper signal component $\hat{\phi}_{ps}(\upsilon,\omega)$ given by equation (16) and that $\hat{\phi}_N(\upsilon,\omega)$ is equal to the sum of the Wiener spectrums of the aliased noise $\hat{\phi}_{an}(\upsilon,\omega)$, electronic noise $\hat{\phi}'_{en}(\upsilon)$, and quantization noise $\hat{\phi}_{\kappa n}(\upsilon,\omega)$ given by equations (17), (18), and (19), respectively. Substituting these results into equation (12) leads to the desired expression for the information density of the signal generated by the optical-mechanical line-scan imaging process:

$$h_i = \frac{1}{2}\iint_{\hat{F}} \log_2\left[1 + \frac{\hat{\phi}_o(\upsilon,\omega)\left|\hat{\tau}_c(\upsilon,\omega)\right|^2}{\sum_{\substack{m=-\infty \\ (m,n)\neq(0,0)}}^{\infty}\sum_{n=-\infty}^{\infty} \hat{\phi}_o\left(\upsilon-\frac{m}{X},\omega-\frac{n}{Y}\right)\left|\hat{\tau}_c\left(\upsilon-\frac{m}{X},\omega-\frac{n}{Y}\right)\right|^2 + K^{-2}\,\hat{\phi}_{en}(\upsilon)\left|\hat{\tau}_e(\upsilon)\right|^2 + \frac{1}{3}\kappa^{-2}}\right] d\upsilon\, d\omega \qquad (20)$$

In order to support the treatment of quantization as additive noise and, hence, to explore the validity of equation (20), consider the following idealized situation. Let the Wiener spectrum of the camera signal with an effective range of $2K$ be

$$K^2\hat{\phi}_o(\upsilon,\omega)\left|\hat{\tau}_c(\upsilon,\omega)\right|^2 = \frac{K^2}{4} \qquad \left(|\upsilon| \leq \frac{1}{2X},\ |\omega| \leq \frac{1}{2Y}\right)$$

$$= 0 \qquad \text{(Elsewhere)}$$

Consequently, the camera passband and sampling passband are the same (i.e., $\hat{B} = \hat{F}$), and the aliasing noise term is zero. Similarly, let the Wiener spectrum of the electronic noise with an effective range $2n_e$ be

$$\phi_{en}(\upsilon)\left|\tau_e(\upsilon)\right|^2 = \frac{n_e^2}{4} \qquad \left(|\upsilon| \leq \frac{1}{2X}\right)$$

$$= 0 \qquad \text{(Elsewhere)}$$

Equation (20) reduces then to

$$h_i = \frac{1}{2}\iint_{\hat{B}} \log_2\left[1 + \frac{1}{\left(\frac{K}{n_e}\right)^{-2} + \frac{4}{3}\kappa^{-2}}\right] d\upsilon\, d\omega$$

Finally, let the electronic noise be small compared to the quantization interval; that is,

$$\left(\frac{K}{\kappa}\right)^2 >> n_e^2$$

Then, equation (20) reduces further to

$$h_i = \frac{1}{2}\iint_{\hat{B}} \log_2\left(1 + \frac{3}{4}\kappa^2\right) d\upsilon\, d\omega = \frac{1}{2XY}\log_2\left(1 + \frac{3}{4}\kappa^2\right)$$

If the number of quantization levels is large, then for this idealized situation

$$h_i \approx \frac{1}{2XY}\log_2\frac{3}{4}\kappa^2 = \frac{1}{XY}\log_2\sqrt{\frac{3}{4}}\,\kappa$$

It is readily recognized that in this situation the information density h_i approaches – but remains slightly less than – the data density h_d given by equation (4a). The fact that the maximum possible value of the ratio h_i/h_d is slightly less than unity is consistent with the observation that h_d represents the maximum possible information density for a spatial radiance distribution which is uniform rather than Gaussian.

It is also informative to compare equation (20) with the general expression for information density derived by Fellgett and Linfoot (ref. 4, p. 399) for film-camera images as given here in the notation of this report:

$$h_{i,film} = \frac{1}{2}\iint_{\hat{F}} \log_2\left[1 + \frac{\hat{\phi}_o(\upsilon,\omega)\left|\hat{\tau}_{lf}(\upsilon,\omega)\right|^2}{\hat{\phi}_p(\upsilon,\omega)\left|\hat{\tau}_{lf}(\upsilon,\omega)\right|^2 + \hat{\phi}_f(\upsilon,\omega)}\right] d\upsilon\, d\omega$$

where $\hat{\phi}_o(\upsilon,\omega)$, $\hat{\phi}_p(\upsilon,\omega)$, and $\hat{\phi}_f(\upsilon,\omega)$ are the Wiener spectrum of the object radiance, photon noise, and film granularity, respectively, and $\hat{\tau}_{lf}(\upsilon,\omega)$ is the combined frequency response of the camera lens and film. It should be noted in particular that photon noise and aliased noise are similarly treated. Both are part of the object radiation, yet appear as statistically independent quantities. Furthermore, both their Wiener spectrums are modified by the frequency response of the camera.

Information Capacity and Efficiency

The information density h_i formulated by equation (20) is a function of scene as well as camera characteristics. It is convenient to assume here that the Wiener spectrum of the scene is constant out to some frequency beyond the system response $\hat{F}$. (See, for example, ref. 16.) Consistent with the previous assumption that the spatial radiance distribution of the scene $o(\chi,\psi)$ is Gaussian with an effective range of 2, its Wiener spectrum $\hat{\phi}_o(\upsilon,\omega)$ is 1/4. It is also convenient to assume that the Wiener spectrum of the electronic noise is constant within the frequency passband of the electrical filter $\hat{\tau}_e(\upsilon)$, with magnitude $\hat{\phi}_{en}(\upsilon) = n_e^2/4$.

With these assumptions, the (statistical mean) information capacity (in binits per steradian) of the optical-mechanical line-scan imaging process becomes

$$h_i = \frac{1}{2}\iint_{\hat{F}} \log_2\left[1 + \frac{\left|\hat{\tau}_c(\upsilon,\omega)\right|^2}{\sum_{\substack{m=-\infty \\ (m,n)\neq(0,0)}}^{\infty}\sum_{n=-\infty}^{\infty}\left|\hat{\tau}_c\left(\upsilon - \frac{m}{X},\omega - \frac{n}{Y}\right)\right|^2 + K^{-2}\, n_e^2\left|\hat{\tau}_e(\upsilon)\right|^2 + \frac{4}{3}\kappa^{-2}}\right] d\upsilon\, d\omega \qquad (21)$$

The data density (in bits per steradian) that is inevitably associated with this information capacity is given by equation (4a) as

$$h_d = \frac{1}{XY}\log_2 \kappa$$

It can be recognized that the objective to maximize the information capacity h_i without regard to the associated data density h_d would lead to sufficient sampling and very small quantization intervals, and, therefore, to large data requirements. It may often be more desirable either to maximize h_i for a fixed value of h_d or to maximize the ratio h_i/h_d. This ratio will be referred to as information efficiency.

EVALUATION

The foregoing formulation of the information capacity of the optical-mechanical line-scan imaging process was based in part on reasonable considerations of the effect of aliasing and quantization rather than on strictly mathematical grounds. It is, therefore, desirable to demonstrate that these assumptions lead to reasonable results.

Frequency-Response Shapes

The realizability of frequency-response shapes of optical apertures is constrained by the requirement that the aperture transmission is always greater than zero. This constraint may be generalized by noting that any aperture transmission function, being always positive, must have a square root; that is, $\tau(\chi,\psi) = \Upsilon^2(\chi,\psi)$, where $\tau(\chi,\psi)$ is the aperture response and $\Upsilon(\chi,\psi)$ is its square root. Taking the spatial Fourier transform and using the transform properties of the convolution yields

$$\hat{\tau}(\upsilon,\omega) = \int_{-\infty}^{\infty}\int_{-\infty}^{\infty} \hat{\Upsilon}(\upsilon',\omega')\,\hat{\Upsilon}(\upsilon - \upsilon',\omega - \omega')d\upsilon'\, d\omega'$$

In words, any realizable transfer function must, in the spatial-frequency domain, be representable as the convolution of a function with itself. Given any response function, realizable or not (it must, of course, be the transform of a real function), a fully realizable one can be generated simply by convolving it with itself (ref. 17).

The frequency-response characteristics of electrical filters are not similarly constrained. Consequently, the overall frequency response of electro-optical systems can be shaped with greater freedom along the line-scan direction than along the azimuth-stepping direction.

It is convenient here to consider only the simplified frequency-response shapes generated by the function

$$\left.\begin{aligned} \hat{\tau}(\upsilon,\omega) &= 1 - \left(\upsilon^2 + \omega^2\right)^{k/2} && \left(\upsilon^2 + \omega^2 \leq 1\right) \\ &= 0 && \left(\upsilon^2 + \omega^2 > 1\right) \end{aligned}\right\} \tag{22}$$

where $k > 0$. (See fig. 3.) For electrical filters, $\hat{\tau}$ depends only on υ and for large k becomes the approximately rectangular-shaped frequency response of ideal low-pass electrical filters. A cylindrical-shaped frequency response (i.e., the rectangular shape with circular symmetry) is not realizable for optical apertures; however, an approximately cone-shaped frequency response is realizable as can be shown by convolving the cylindrical shape with itself. In fact, this convolution yields the frequency response of a diffraction-limited lens (see, for example, ref. 9), which is approximated by equation (22) for $k = 1$.

The remainder of this paper is concerned with four numerical examples. For convenience, in all but the first example, the camera passband $\hat{F}$ is normalized to be the set of points (υ,ω) with $\upsilon^2 + \omega^2 \leq 1$. Consequently, the Nyquist elevation and azimuth sampling rates are $1/X = 2$ and $1/Y = 2$, respectively. In the first example only an electrical filter is considered for which the Nyquist rate is $1/X = 2$.

Examples

The performance of the optical-mechanical line-scan imaging process for fixed sampling rates ($1/X$ and $1/Y$) is determined – consistent with the assumptions that have been made – by the signal-to-noise ratio K/n_e, the digital encoding level η, the optical filter shape parameter k_o, the electrical filter shape parameter k_e, and the electrical filter cutoff frequency υ_e. Table I presents a summary of values for these five parameters that are used in the following examples.

Electrical filters.- Consider first a one-dimensional example that is representative of electrical filters. The information capacity analogous to equation (21) is

$$h_i = \int_0^{\upsilon_e} \log_2 \left[1 + \frac{\hat{\tau}_e^2(\upsilon)}{\sum\limits_{\substack{m=-\infty \\ m\neq 0}}^{\infty} \hat{\tau}_e^2\left(\upsilon - \frac{m}{X}\right) + \left(\frac{K}{n_e}\right)^{-2} \hat{\tau}_e^2(\upsilon) + \frac{4}{3}\kappa^{-2}} \right] d\upsilon \tag{23}$$

The frequency response of the electrical filter is given by

$$\left.\begin{aligned} \hat{\tau}_e(\upsilon) &= 1 - \left|\frac{\upsilon}{\upsilon_e}\right|^{k_e} && \left(|\upsilon| \leq \upsilon_e\right) \\ &= 0 && \left(|\upsilon| > \upsilon_e\right) \end{aligned}\right\} \tag{24}$$

where υ_e is the cutoff frequency. Analogous to equations (4), the associated data density is

$$h_d = \frac{1}{X} \log_2 \kappa = \frac{\eta}{X} \tag{25}$$

The units of h_i and h_d are binits/radian and bits/radian, respectively.

Often more useful and certainly more familiar is the information rate $\dot{h}_i = \dot{\chi}_s h_i$ binits/second and the data rate $\dot{h}_d = \dot{\chi}_s h_d$ bits/second, where $\dot{\chi}_s$ is the mirror line-scan rate in radians/second. The information efficiency remains the same $\left(\text{i.e., } h_i/h_d = \dot{h}_i/\dot{h}_d\right)$.

Figure 4 illustrates the variation of information capacity h_i, data density h_d, and information efficiency h_i/h_d with sampling rate $1/X$. For reference: $\upsilon_e = 1$; the Nyquist sampling rate is $1/X = 2$ cycles/radian; the root-mean-square (rms) magnitude of the electronic noise is

$$\sqrt{\left(\frac{K}{n_e}\right)^{-2} \int_0^1 \hat{\tau}_e^2(\upsilon)\, d\upsilon} = 1.3 \times 10^{-3}$$

for $K/n_e = 400$ and $k_e = 1$; and the rms magnitude of the quantization noise for $\eta = 8$ bits is

$$\sqrt{\frac{4}{3}\kappa^{-2}} = 2^{-\eta}\sqrt{\frac{4}{3}} = 4.5 \times 10^{-3}$$

The results shown in figure 4 are intuitively satisfying. It should be noted in particular in figure 4(c) that the information efficiency approaches unity $\left(h_i/h_d = 0.9\right)$ for a nearly ideal filter $\left(k_e = 4\right)$ and a nearly Nyquist sampling rate $\left(1/X = 1.95\right)$ and that the peak information efficiency not only decreases with a poorer filter response but also shifts

toward lower sampling rates. Also, note in figure 4(b) that 10-bit encoding provides a significantly higher information capacity over 8-bit encoding, but that the latter provides a slightly higher information efficiency. Finally, note in figure 4(a) that a signal-to-noise ratio significantly higher than $K/n_e = 400$ does not appreciably increase either h_i or h_i/h_d.

Optical filters (symmetric sampling).- Consider next a two-dimensional example with circular symmetry that is representative of optical filters. The information capacity given by equation (21) becomes

$$h_i = 2\int_0^1 \int_0^{\sqrt{1-\omega^2}} \log_2 \left[1 + \sum_{\substack{m=-\infty \\ (m,n)\neq(0,0)}}^{\infty} \sum_{n=-\infty}^{\infty} \frac{\hat{\tau}_o^2(\upsilon,\omega)}{\hat{\tau}_o^2\left(\upsilon - \frac{m}{X}, \omega - \frac{n}{Y}\right) + \left(\frac{K}{n_e}\right)^{-2} + \frac{4}{3}\kappa^{-2}} \right] d\upsilon\, d\omega \qquad (26)$$

The frequency response of the optical filter is given by

$$\left.\begin{aligned} \hat{\tau}_o(\upsilon,\omega) &= 1 - \left(\upsilon^2 + \omega^2\right)^{k_o/2} && \left(\upsilon^2 + \omega^2 \leq 1\right) \\ &= 0 && \left(\upsilon^2 + \omega^2 > 1\right) \end{aligned}\right\} \qquad (27)$$

The associated data density given in equations (4) is

$$h_d = \frac{1}{XY} \log_2 \kappa = \frac{\eta}{XY}$$

The units of h_i and h_d are binits/steradian and bits/steradian, respectively.

Results for h_i, h_d, and h_i/h_d are plotted in figure 5 for symmetric elevation and azimuth sampling rates (i.e., $1/X = 1/Y$). It should be noted by comparing figures 4 and 5 that the information efficiency for optical filters tends to be substantially lower than for electrical filters. Also, the peak information efficiency tends to occur at substantially lower sampling rates than the Nyquist sampling rate $1/X = 1/Y = 2$.

Optical filters (unsymmetric sampling).- Consider next a two-dimensional example identical to the previous one except that the elevation and azimuth sampling rates, $1/X$ and $1/Y$, respectively, are not restricted to be equal. Since the information capacity h_i and efficiency h_i/h_d are then functions of two sampling rates, it is necessary to use a two-dimensional graphical representation of numerical solutions. Figure 6 presents a contour plot of information efficiency $\left(\text{i.e., lines of constant } h_i/h_d\right)$ corresponding to the set of parameters $K/n_e = 400$, $\eta = 8$ bits, and $k_o = 1$. As would be expected, the contour lines have diagonal symmetry for a filter with circular symmetry. Consequently, the maximum information efficiency is obtained with symmetric sampling rates (i.e., $I/X = I/Y$).

Figure 7(a) presents a contour plot of information capacity h_i and three contours of constant data density h_d. Figure 7(b) presents a plot of values of h_i along the three contours of constant h_d against the azimuth sampling rate $1/Y$. Again, the maximum information capacity is obtained with symmetric sampling rates.

Electro-optical systems.- Consider last a two-dimensional example without circular symmetry that is representative of electro-optical systems. The information capacity becomes

$$h_i = 2\int_0^1 \int_0^{\sqrt{1-\omega^2}} \log_2 \left[1 + \frac{\hat{\tau}_o^2(\upsilon,\omega)\,\hat{\tau}_e^2(\upsilon)}{\sum_{\substack{m=-\infty \\ (m,n)\neq(0,0)}}^{\infty} \sum_{n=-\infty}^{\infty} \hat{\tau}_o^2\left(\upsilon - \frac{m}{X}, \omega - \frac{n}{Y}\right) \hat{\tau}_e^2\left(\upsilon - \frac{m}{X}\right) + \left(\frac{K}{n_e}\right)^{-2} \hat{\tau}_e^2(\upsilon) + \frac{4}{3}\kappa^{-2}} \right] d\upsilon\, d\omega \tag{28}$$

The frequency response of the electrical filter is given by equations (24) and of the optical filter by equations (27). The associated data density h_d is given by equations (4).

Figure 8 presents a contour plot of the information efficiency h_i/h_d analogous to figure 6, but for $K/n_e = 400$, $\eta = 8$ bits, $k_o = 1$, $k_e = 4$, and $\upsilon_e = 0.8$. Maximum values of h_i/h_d still occur at sampling rates below the Nyquist rate. However, as would be expected, the location of these maximum values occurs off the diagonal at an elevation sampling rate which is lower than the azimuth sampling rate because of the additional electrical filtering along the elevation direction.

Figure 9 presents information-capacity plots analogous to figure 7. Again, as in figure 8, the maximum information capacity for a fixed data density occurs at an elevation sampling rate lower than the azimuth sampling rate.

CONCLUDING REMARKS

Imaging systems cannot exactly reproduce a scene as an image. All images are degraded at least by some blurring of small detail and by random noise. As demonstrated by Fellgett and Linfoot, these two phenomena inevitably limit the amount of information density in an image. The optical-mechanical line-scan imaging process of many space-borne cameras almost unavoidably generates some additional image degradation due to aliasing and quantization. The results of Fellgett and Linfoot are extended here to include the effects of these degradations. All formulations are constrained by the assumption of statistically independent and additive Gaussian random processes, as have been all previous related analyses for incoherent radiation. This assumption includes here in particular the treatment of aliasing and quantization as noise sources.

The information density in an image depends not only on characteristics of the imaging system but also on statistical properties of the scene; namely, its random spatial radiance variation and power spectral density (i.e., Wiener spectrum). It is assumed that the radiance variation is Gaussian and that the Wiener spectrum is flat out to some spatial frequency beyond the optical passband of the imaging system. The information density of an image is then solely determined by the information capacity of the instrument used to obtain this image.

The objective to maximize the information capacity of the optical-mechanical line-scan imaging process without regard to the associated data density can lead to impractically large data requirements. It may be preferable either to maximize the information capacity for a fixed data density or to maximize the information efficiency (i.e., the ratio of information capacity to data density). Both the information capacity for a fixed data density and the information efficiency exhibit a distinct single maximum when displayed as a function of sampling rate.

It is shown that the information efficiency of an instrument can approach unity (i.e., that the information capacity of an instrument can approach the data density) under certain theoretical conditions. These conditions can be approximated in practice by electronic systems for time-varying signals but not by optical systems for space-varying signals. The reason for this is that the frequency response of electronic systems can approach a rectangular shape, whereas that of optical systems cannot approach a two-dimensional equivalent to this shape (i.e., a cylinderlike shape). In fact, the frequency response of an optical system is in practice generally limited by the conelike shape of a diffraction-limited lens, limiting the information efficiency of optical-mechanical line-scan devices to considerably less than unity. Nevertheless, within this limit, the information efficiency can vary significantly with sampling rate, signal-to-noise ratio, and quantization interval, as has been illustrated for a wide range of reasonable camera frequency-response shapes.

Langley Research Center,
National Aeronautics and Space Administration,
Hampton, Va., April 22, 1975.

REFERENCES

1. Selivanov, A. S.; Govorov, V. M.; Titov, A. S.; and Chemodanov, V. P.: Lunar Station Television Camera. Contract NAS 7-100, Reilly Translations, 1968. (Available as NASA CR-97884.)

2. Selivanov, A. S.; Govorov, V. M.; Zasetskii, V. V.; and Timokhin, V. A. (Morris D. Friedman, transl.): Chapter V. Peculiarities of the Construction and Fundamental Parameters of the "Lunokhod-1" Television Systems. Lockheed Missiles & Space Co. Transl. (From Peredvizhenaia Laboratoriia na Lune – Lunokhod-1, Acad. Sci. SSSR Press (Moscow), 1971, pp. 55-64.)

3. Mutch, T. A.; Binder, A. B.; Huck, F. O.; Levinthal, E. C.; Morris, E. C.; Sagan, Carl; and Young, A. T.: Imaging Experiment: The Viking Lander. Icarus, vol. 16, no. 1, Feb. 1972, pp. 92-110.

4. Fellgett, P. B.; and Linfoot, E. H.: On the Assessment of Optical Images. Phil. Trans. Roy. Soc. London, ser. A, vol. 247, no. 931, Feb. 17, 1955, pp. 369-407.

5. Shannon, C. E.: A Mathematical Theory of Communication. Bell Syst. Tech. J., vol. XXVII, no. 3, July 1948, pp. 379-423.

6. Huck, Friedrich O.; Wall, Stephen D.; and Burcher, Ernest E.: An Investigation of the Facsimile Camera Response to Object Motion. NASA TN D-7668, 1974.

7. Bracewell, R.: The Fourier Transform and Its Applications. McGraw-Hill Book Co., Inc., c.1965.

8. Goodman, Joseph W.: Introduction to Fourier Optics. McGraw-Hill Book Co., Inc., 1968.

9. Huck, Friedrich O.; and Lambiotte, Jules J., Jr.: A Performance Analysis of the Optical-Mechanical Scanner As an Imaging System for Planetary Landers. NASA TN D-5552, 1969.

10. Linfoot, E. H.: Information Theory and Optical Images. J. Opt. Soc. of America, vol. 45, no. 10, Oct. 1955, pp. 808-819.

11. Linfoot, E. H.: Fourier Methods in Optical Image Evaluation. The Focal Press, c.1964.

12. Lee, Y. W.: Statistical Theory of Communication. John Wiley & Sons, Inc., c.1960.

13. Jones, R. Clark: Information Capacity of Radiation Detectors. J. Opt. Soc. of America, vol. 50, no. 12, Dec. 1960, pp. 1166-1170.

14. Blackman, R. B.; and Tukey, J. W.: The Measurement of Power Spectra. Dover Publ., Inc., 1959.

15. Carlson, A. Bruce: Communications Systems. McGraw-Hill Book Co., c.1968.

16. O' Neill, Edward L.: Introduction to Statistical Optics. Addison-Wesley Pub. Co., Inc., c.1963.

17. Katzberg, Stephen J.; Huck, Friedrich O.; and Wall, Stephen D.: Photosensor Aperture Shaping To Reduce Aliasing in Optical-Mechanical Line-Scan Imaging Systems. Appl. Optics, vol. 12, no. 5, May 1973, pp. 1054-1060.

TABLE I.- SUMMARY OF EXAMPLES

Systems	Parameters				
	K/n_e	η, bits	k_o	k_e	υ_e
Electrical filter	100	6	Not applicable	0.25	1
	400	8		1	1
	1600	10		4	1
Optical filter, symmetric sampling	100	6	0.25	Not applicable	
	400	8	.5		
	1600	10	1		
Optical filter, unsymmetric sampling	400	8	1	Not applicable	
Electro-optical filter, unsymmetric sampling	400	8	1	4	0.8

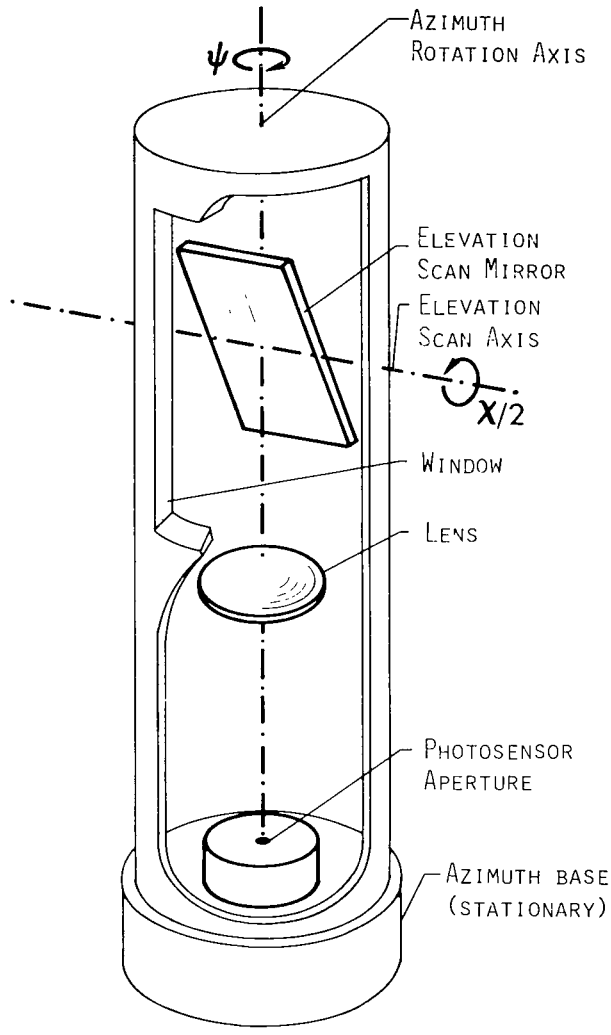

Figure 1.- Basic facsimile-camera configuration.

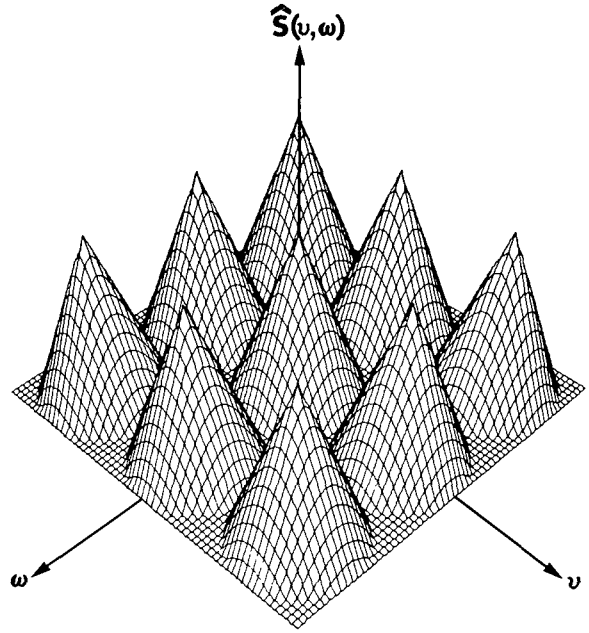

(a) Sufficient sampling.

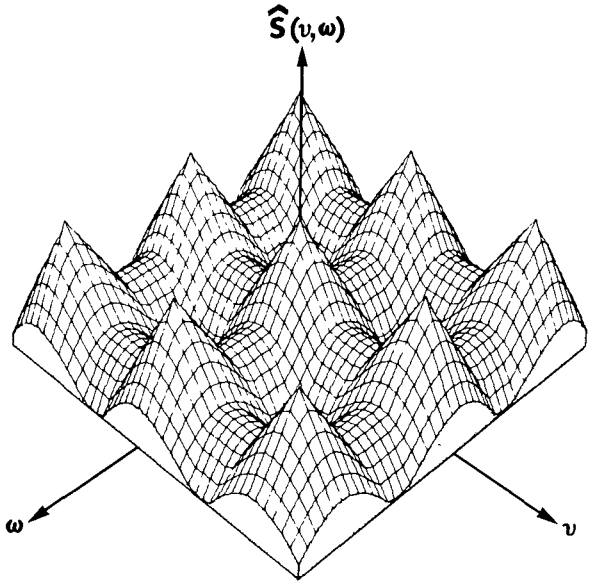

(b) Insufficient sampling.

Figure 2.- Frequency spectrum generated by the optical-mechanical line-scan imaging process.

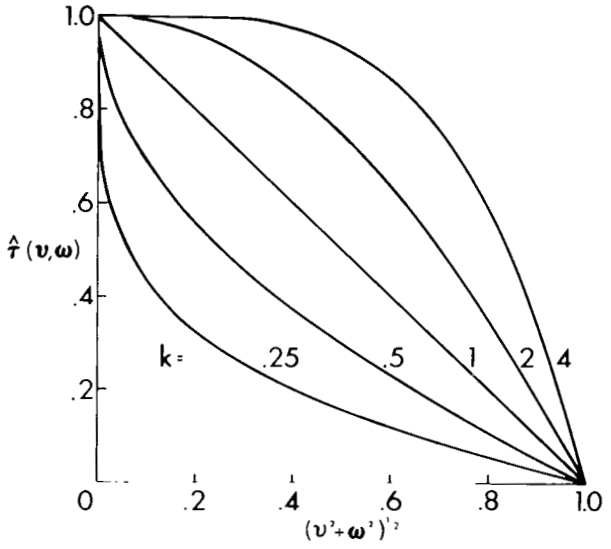

Figure 3.- Simplified frequency-response shapes.

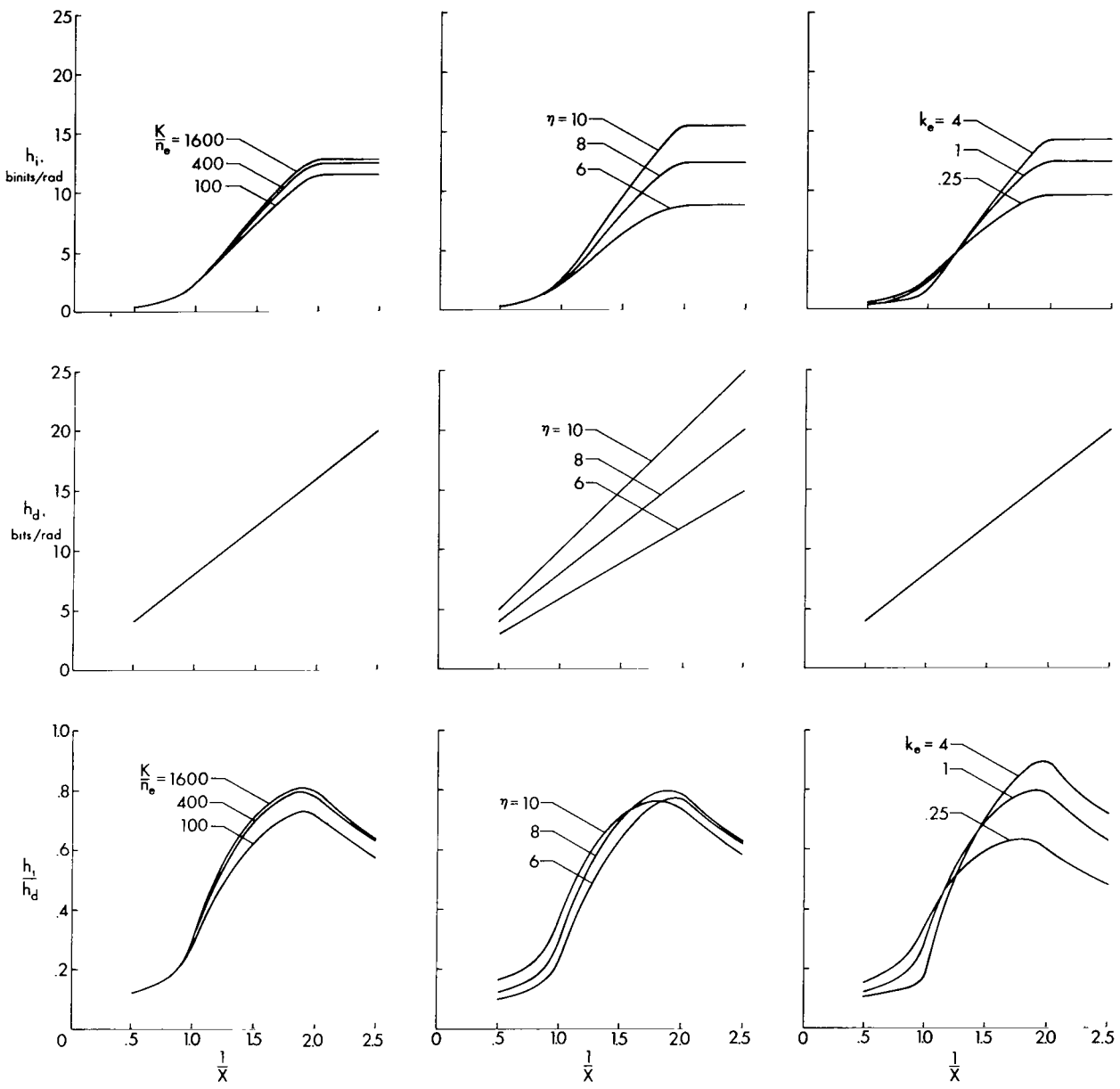

(a) $k_e = 1$; $\eta = 8$ bits.

(b) $K/n_e = 400$; $k_e = 1$.

(c) $K/n_e = 400$; $\eta = 8$ bits.

Figure 4.- Variation of information capacity h_i, data density h_d, and information efficiency h_i/h_d with sampling rate $1/X$ for electrical filters.

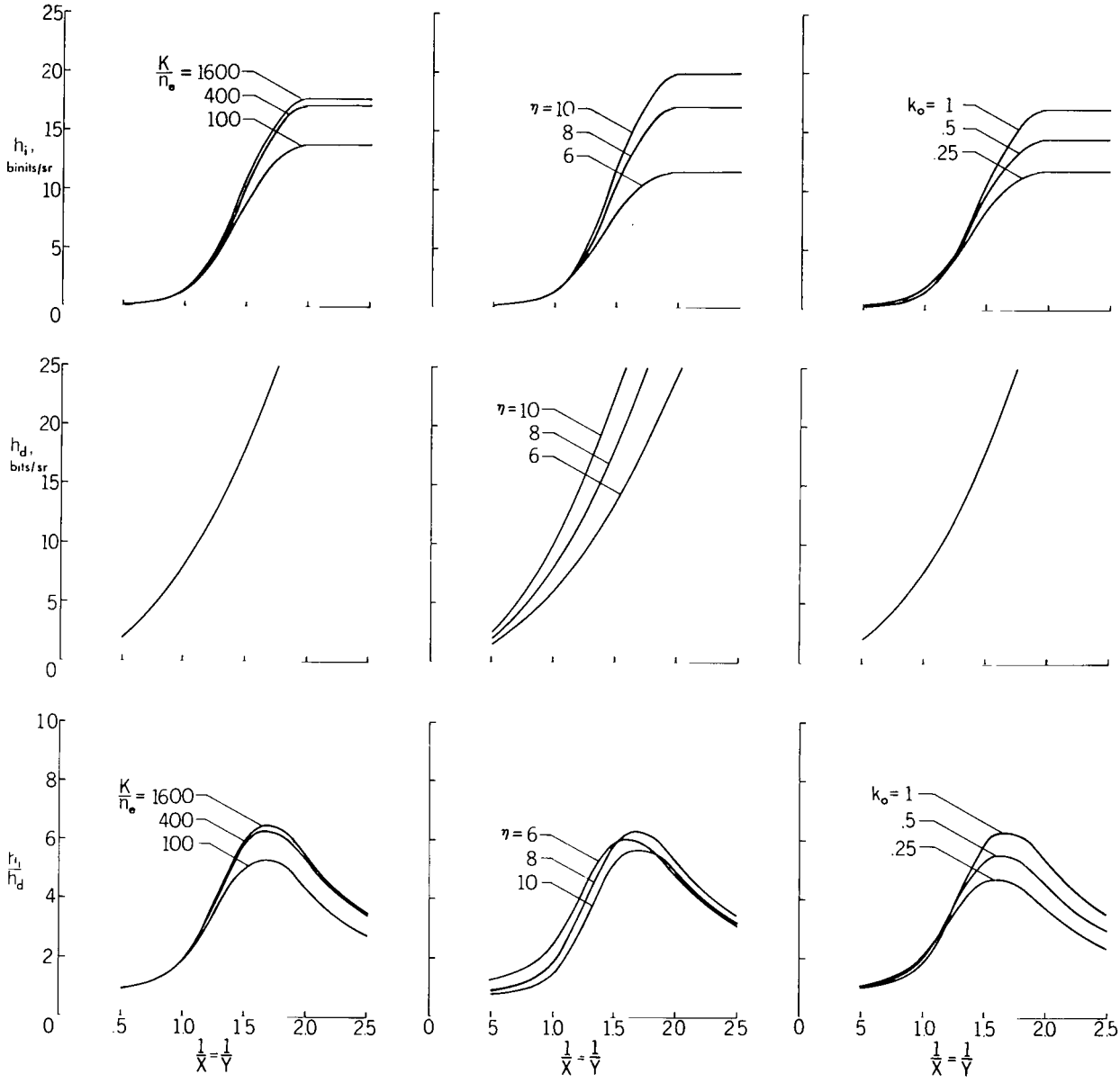

(a) $k_o = 1$; $\eta = 8$ bits.

(b) $K/n_e = 400$; $k_o = 1$.

(c) $K/n_e = 400$; $\eta = 8$ bits.

Figure 5.- Variation of information capacity h_i, data density h_d, and information efficiency h_i/h_d with symmetric sampling rates $1/X = 1/Y$ for optical filters.

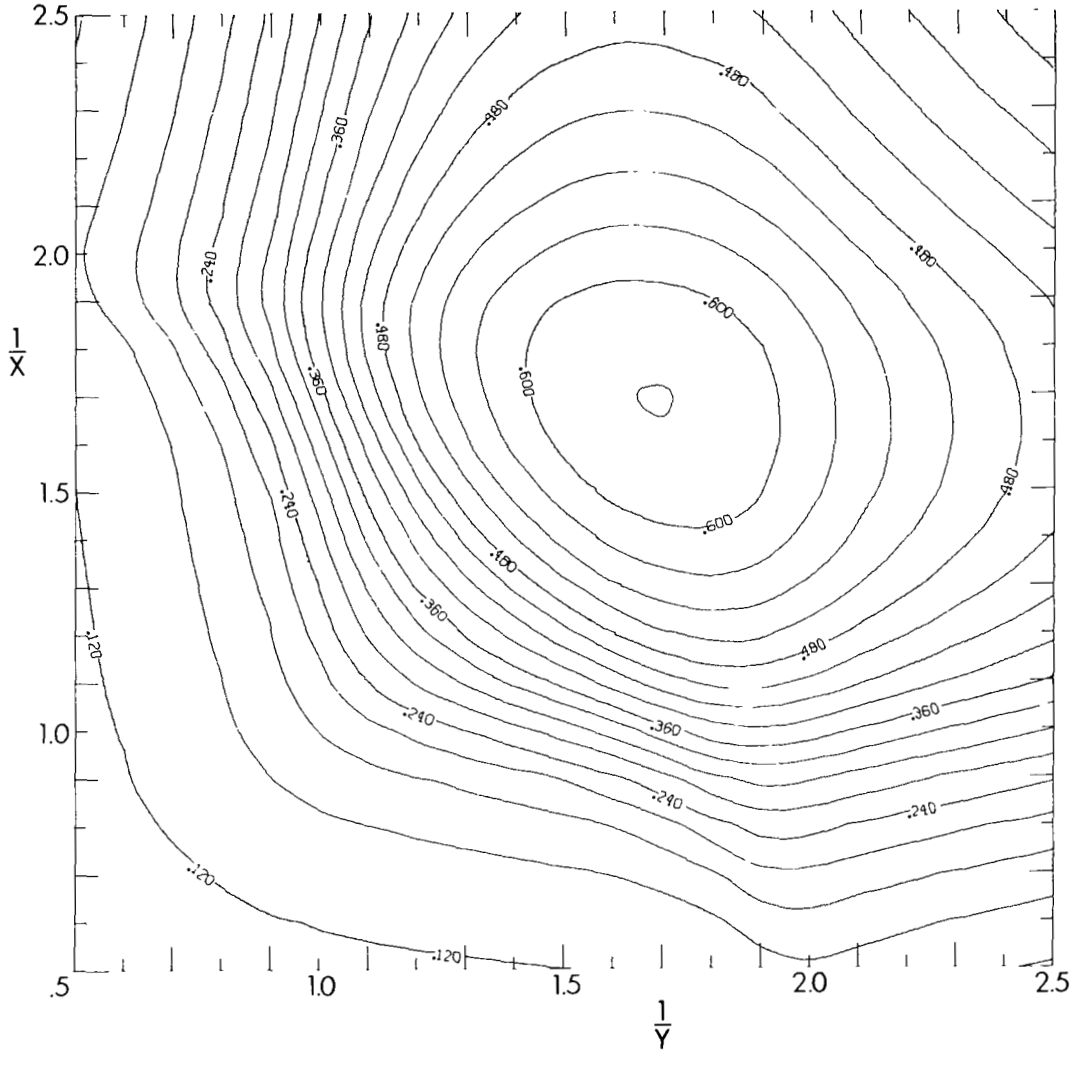

Figure 6.- Contour plot of information efficiency h_i/h_d as a function of sampling rates 1/X and 1/Y for optical filters. $K/n_e = 400$; $\eta = 8$ bits; and $k_o = 1$.

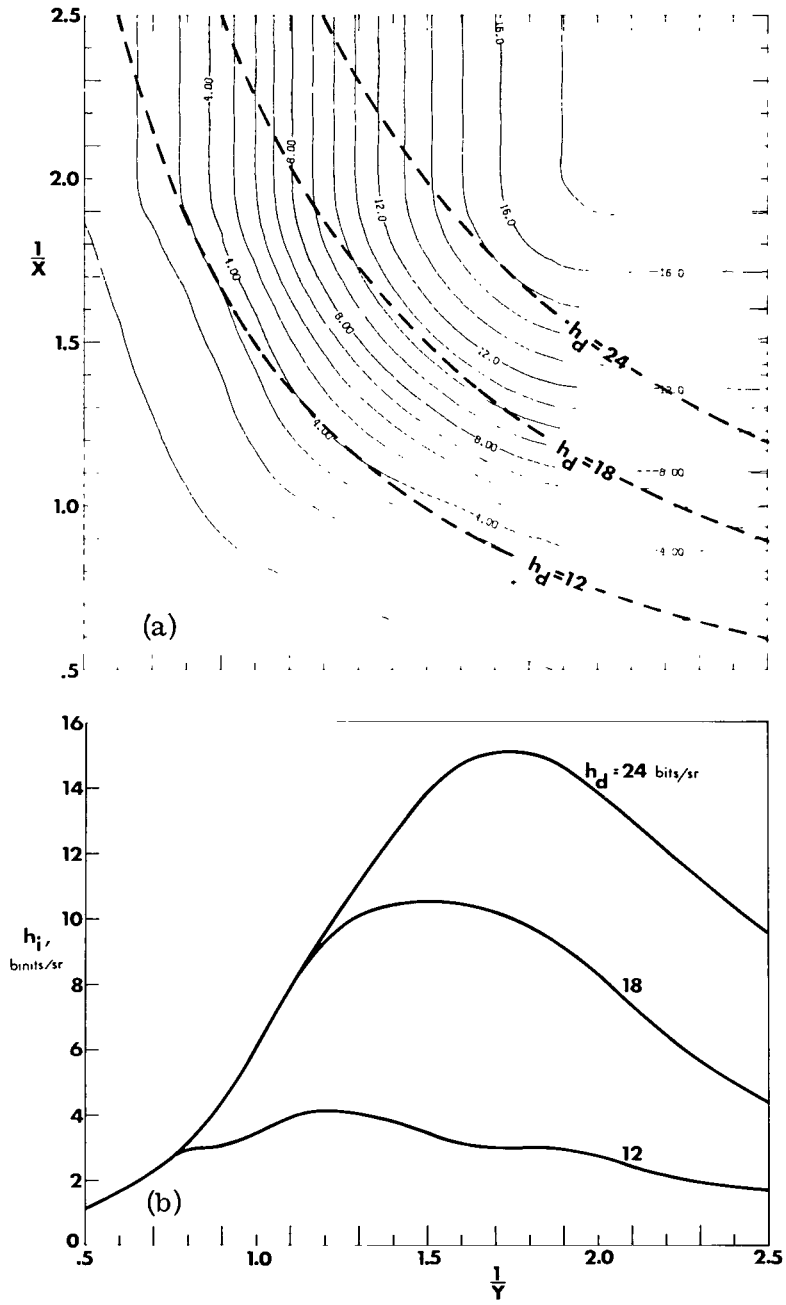

(a) Contour plot of information capacity h_i and three contours of constant data density h_d as a function of sampling rates 1/X and 1/Y.

(b) Plot of h_i along the three contours of constant h_d against sampling rate 1/Y.

Figure 7.- Plots of information capacity for optical filters. $K/n_e = 400$; $\eta = 8$ bits; and $k_o = 1$.

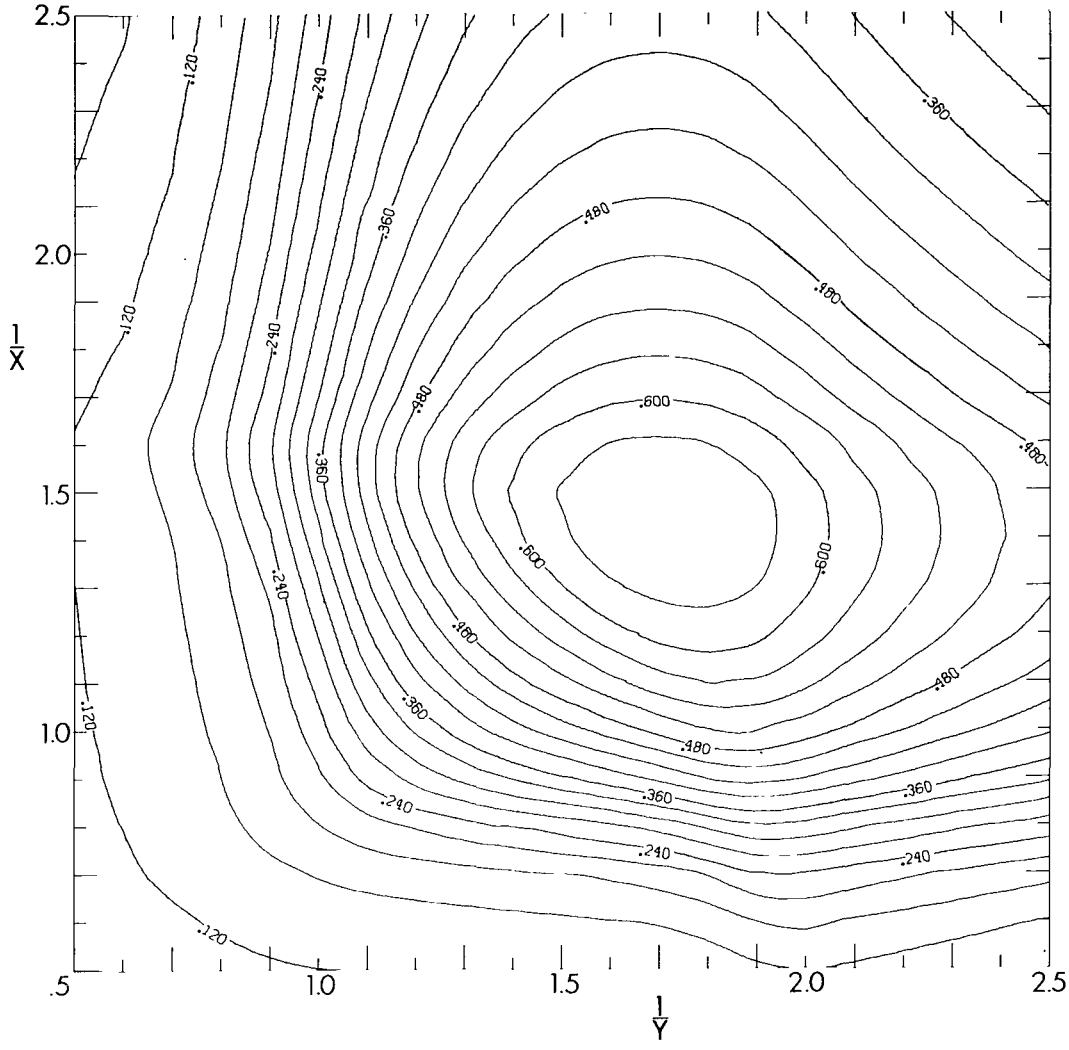

Figure 8.- Contour plot of information efficiency h_i/h_d as a function of sampling rates 1/X and 1/Y for electro-optical systems. $K/n_e = 400$; $\eta = 8$ bits; $k_o = 1$; $k_e = 4$; and $\upsilon_e = 0.8$.

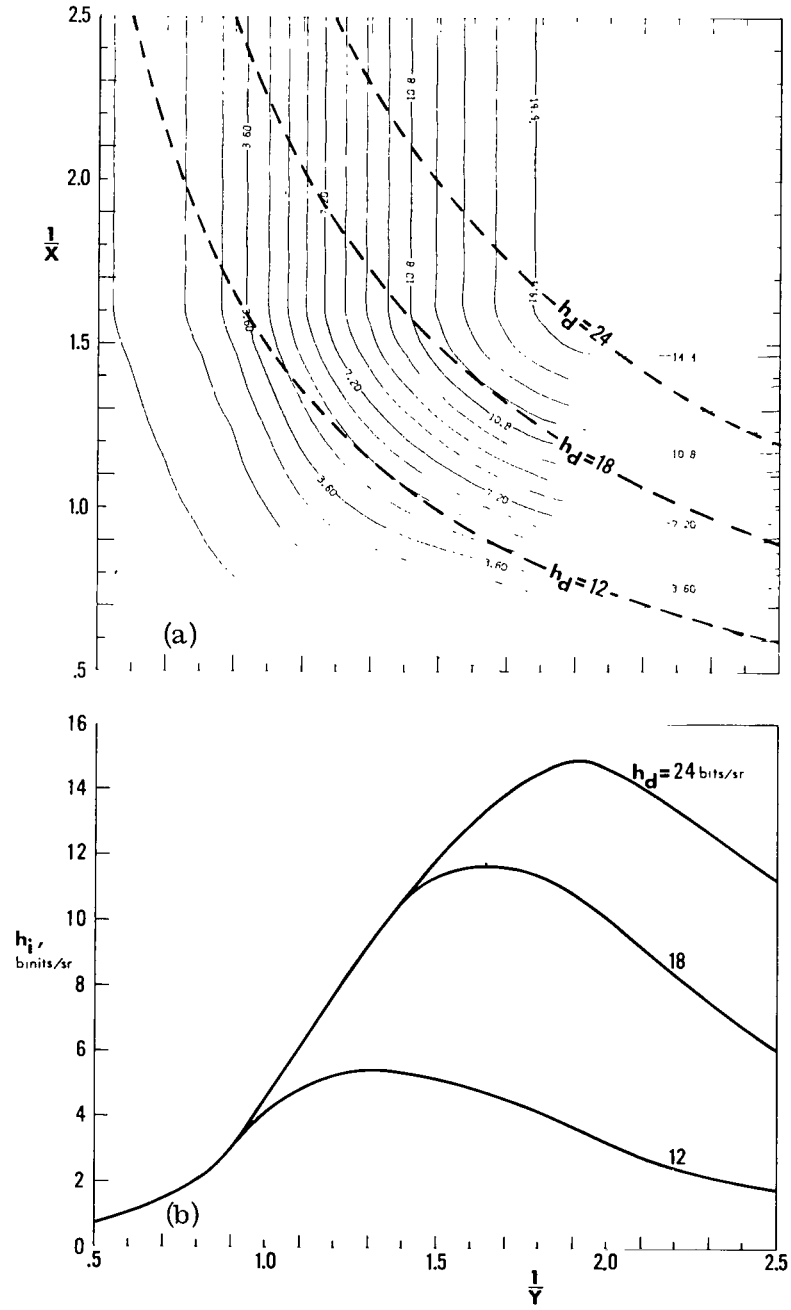

(a) Contour plot of information capacity h_i and three contours of constant data density h_d as a function of sampling rates $1/X$ and $1/Y$.

(b) Plot of h_i along the three contours of constant h_d against sampling rate $1/Y$.

Figure 9.- Plots of information capacity for electro-optical systems. $K/n_e = 400$; $\eta = 8$ bits; $k_o = 1$; $k_e = 4$; and $\upsilon_e = 0.8$.

"The aeronautical and space activities of the United States shall be conducted so as to contribute . . . to the expansion of human knowledge of phenomena in the atmosphere and space. The Administration shall provide for the widest practicable and appropriate dissemination of information concerning its activities and the results thereof."

—NATIONAL AERONAUTICS AND SPACE ACT OF 1958

NASA SCIENTIFIC AND TECHNICAL PUBLICATIONS

TECHNICAL REPORTS: Scientific and technical information considered important, complete, and a lasting contribution to existing knowledge.

TECHNICAL NOTES: Information less broad in scope but nevertheless of importance as a contribution to existing knowledge.

TECHNICAL MEMORANDUMS: Information receiving limited distribution because of preliminary data, security classification, or other reasons. Also includes conference proceedings with either limited or unlimited distribution.

CONTRACTOR REPORTS: Scientific and technical information generated under a NASA contract or grant and considered an important contribution to existing knowledge.

TECHNICAL TRANSLATIONS: Information published in a foreign language considered to merit NASA distribution in English.

SPECIAL PUBLICATIONS: Information derived from or of value to NASA activities. Publications include final reports of major projects, monographs, data compilations, handbooks, sourcebooks, and special bibliographies.

TECHNOLOGY UTILIZATION PUBLICATIONS: Information on technology used by NASA that may be of particular interest in commercial and other non-aerospace applications. Publications include Tech Briefs, Technology Utilization Reports and Technology Surveys.

Details on the availability of these publications may be obtained from:

SCIENTIFIC AND TECHNICAL INFORMATION OFFICE

NATIONAL AERONAUTICS AND SPACE ADMINISTRATION

Washington, D.C. 20546